THE GERONTOLOGICAL SOCIETY OF AMERICA®

Journals of Gerontology: Biological Sciences
cite as: *J Gerontol A Biol Sci Med Sci*, 2022, Vol. 77, No. 10, 1969–1974
https://doi.org/10.1093/gerona/glac091
Advance Access publication April 24, 2022

OXFORD

Research Practice

The Aging Human Lung Mucosa: A Proteomics Study

Andreu Garcia-Vilanova, Bsc,[1,*] Angélica M. Olmo-Fontánez, MS,[1,2] Juan I. Moliva, PhD,[3] Anna Allué-Guardia, PhD,[1] Harjinder Singh, MD,[4] Robert E. Merritt, MD,[5] Diego J. Maselli, MD,[4] Jay I. Peters, MD,[4] Blanca I. Restrepo, PhD,[6] Yufeng Wang, PhD,[7] Larry S. Schlesinger, MD,[1] Joanne Turner, PhD,[1] Susan T. Weintraub, PhD,[8] and Jordi B. Torrelles, PhD[1]

[1]Population Health and Host Pathogen Interactions Programs, Texas Biomedical Research Institute, San Antonio, Texas, USA. [2]Integrated Biomedical Sciences Program, The University of Texas Health Science Center, San Antonio, Texas, USA. [3]Vaccine Research Center, National Institute of Allergy and Infectious Diseases, National Institutes of Health, Bethesda, Maryland, USA. [4]Division of Pulmonary and Critical Care Medicine, School of Medicine, UT Health San Antonio, San Antonio, Texas, USA. [5]Department of Surgery, College of Medicine, The Ohio State University, Columbus, Ohio, USA. [6]UT Health Houston, School of Public Health, Brownsville, Texas, USA. [7]Department of Molecular Microbiology and Immunology, South Texas Center for Emerging Infectious Diseases, UTSA, San Antonio, Texas, USA. [8]Department of Biochemistry and Structural Biology, UT Health San Antonio, San Antonio, Texas, USA.

*Address correspondence to: Jordi B. Torrelles, 8715 W Military Dr, San Antonio, 78227 TX, USA. E-mail: agarciavilanova@txbiomed.org

Received: October 6, 2021; Editorial Decision Date: April 6, 2022

Decision Editor: David Le Couteur, MBBS, FRACP, PhD

Abstract

The older adult population, estimated to double by 2050, is at increased risk of respiratory infections and other pulmonary diseases. Biochemical changes in the lung alveolar lining fluid (ALF) and in alveolar compartment cells can alter local immune responses as we age, generating opportunities for invading pathogens to establish successful infections. Indeed, the lung alveolar space of older adults is a pro-inflammatory, pro-oxidative, dysregulated environment that remains understudied. We performed an exploratory, quantitative proteomic profiling of the soluble proteins present in ALF, developing insight into molecular fingerprints, pathways, and regulatory networks that characterize the alveolar space in old age, comparing it to that of younger individuals. We identified 457 proteins that were significantly differentially expressed in older adult ALF, including increased production of matrix metalloproteinases, markers of cellular senescence, antimicrobials, and proteins of neutrophilic granule origin, among others, suggesting that neutrophils in the lungs of older adults could be potential contributors to the dysregulated alveolar environment with increasing age. Finally, we describe a hypothetical regulatory network mediated by the serum response factor that could explain the neutrophilic profile observed in the older adult population.

Keywords: Alveolar lining fluid, Mass spectrometry, Respiratory diseases, Comparative proteomics

It is estimated that by 2050, the worldwide population of individuals who are 65 years and older will have nearly doubled to 22% of the population. The process of aging is associated with innate and adaptive immune dysfunction, increased basal tissue inflammation, and cellular metabolic dysregulation, commonly referred to as "inflammaging." This process leads to increased susceptibility to respiratory infections, one of the top causes of death globally in older adults.

The lung alveolar mucosa, comprised of a surfactant lipid layer and an aqueous hypophase rich in soluble proteins, defined as alveolar lining fluid (ALF), is constantly produced and recycled by Type II alveolar epithelial cells (AT-IIs) (1). We hypothesized that during the continuum of aging, there is an alteration of the phenotype and function of AT-IIs and other lung cells and that these changes negatively affect the composition, function, and innate immune responses of the alveolar mucosa. This is of relevance, since this is the site of first contact between external pathogens and host cells.

Our previous studies have demonstrated that the older adult lung constitutes a pro-oxidative and pro-inflammatory environment, with altered levels and function of complement and surfactant proteins (2). As a consequence, exposure of the intracellular pathogen *Mycobacterium tuberculosis* (*M.tb*) to older adult ALF results in increased *M.tb* intracellular growth in vitro and in vivo (3,4).

In-depth studies of the biochemical composition and inflammatory status of ALF in the older adult human population are scarce, due to the difficulty in obtaining viable samples for analysis. Understanding the biochemical composition of ALF in older adults should provide valuable insight into the changes that occur during aging in the lung. By comparing ALF proteomic profiles from older adult humans to those from younger individuals, we identified individual molecules, networks, and pathway regulators that are altered significantly in the older adult ALF. We discuss how these differences may be responsible for the susceptibility to respiratory infections observed in the older adult population, with an emphasis on a significant signature of neutrophil-mediated basal inflammation.

Results

Comparative Mass Spectrometry-Based Proteomic Analysis of Human E-ALF Versus A-ALF

We performed data-independent acquisition mass spectrometry (DIA-MS) to identify and determine relative amounts of proteins in human ALF from 6 adults (≤48 years old, A-ALF) and 10 older adults (≥62 years old, E-ALF). A total of 2 239 proteins were identified; of these, 1,771 proteins had over 2 quantified peptides (Figure 1A). We further identified differentially expressed proteins (DEPs) from the older adult group that we deemed relevant for this exploratory study, using $p < .055$ as the cutoff based on the Benjamini–Hochberg multiple corrections control of FDR $q < 0.20$, as described (5), and $\log_2$-transformed fold-change ≤–0.5 and ≥0.5, yielding 457 DEPs of interest. Of these, 217 DEPs were significantly higher in E-ALF (Supplementary Table 1, $\log_2$ fold changes), 156 were at $p < .05$; 46 at $p < .005$; 9 at $p < .0005$ (ASSY, CALU, CAN2, CAPS2, CPNS1, NASP, PAPS1, PGRP1, and SPB10), and 6 at $p < .0001$ (ECP, IGHM, MMP-9, NCHL1, RSH4A, and S100P). E-ALF also presented 240 DEPs significantly lower (Supplementary Table 2, $\log_2$ fold changes), 133 were at $p < .05$; 76 at $p < .005$; 23 at $p < .0005$ (ARC1B, ARP2, ARP3, ARPC5, CSRP1, DIAP1, EMAL4, IFTI3, IST1, KPCD, MK14, MOES, NCF4, PANC2, PLCG2, PLEK, SARG, SNX5, SYVC, UPP1, VAT1, VATE1, and URP2) and 8 at $p < .0001$ (BAX, CLIC4, COR1C, FHL1, FLNA, FLNC, PTN6, and THMS2). Of the total proteins identified, approximately 30% were annotated as being of intracellular origin. Cluster analysis confirmed that the sample variability observed was driven by the donor age group (Figure 1B).

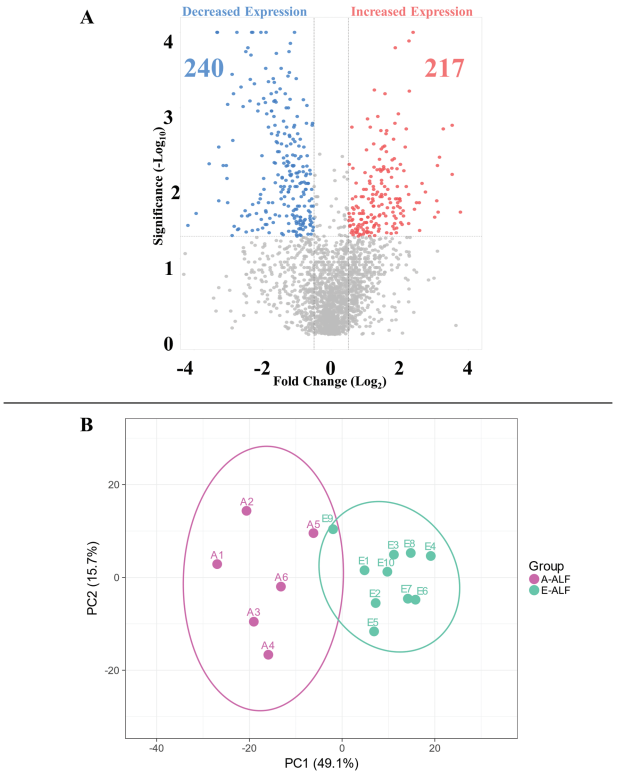

Figure 1. (**A**) Volcano plot of the distribution of differentially expressed proteins (DEPs) in E-ALF versus A-ALF. The *x*-axis shows $\log_2$-transformed protein fold changes for human E-ALF versus A-ALF, the *y*-axis shows $-\log_{10}$-transformed *p*-values. A total of 457 DEPs were identified, 217 being higher (red), and 240 being lower (blue) in E-ALF. (**B**) Principal component analysis of sample distribution. A-ALF (pink) and E-ALF (aqua) 95% confidence intervals (circles) and individual sample labels shown. Full color version is available within the online issue.

Gene Ontology (GO) Enrichment Analysis of Human E-ALF Versus A-ALF

GO annotations and classifications were determined for the 457 identified DEPs in E-ALF versus A-ALF (Supplementary Figure 1, top). A summary of the GO annotations for all detected proteins regardless of their significance between E-ALFs and A-ALFs is provided in Supplementary Figure 1, bottom.

Top Identified Canonical Pathways Enriched in Human E-ALF Versus A-ALF

We used Ingenuity Pathway Analysis (IPA, Qiagen) to identify the top canonical pathways overrepresented by the identified DEPs. The top 40 significantly overrepresented pathways in E-ALFs versus A-ALF (Figure 2, selected by the highest *p*-values of overlap) were defined by the right-tailed Fisher's exact test (–log *p*-values > 4.02). Pathways with the highest –log *p*-values were *Actin Cytoskeleton Signaling*, *Remodeling of Epithelial Adherens Junction*, and *Integrin Signaling*. Values for the ratio of pathway proteins (DEPs in dataset belonging to pathway/Proteins in the pathway for reference dataset) are provided as the dot size, with the highest ratios found for *UDP-N-acetyl-D-galactosamine Biosynthesis II*, *Remodeling of Epithelial Adherens Junction*, and *tRNA charging*. Finally, the activation *z*-score, a prediction of the overall activation state of a pathway based on the status of detected proteins, is shown by the bubble position on the x-axis, with the biggest changes being observed for *Signaling by Rho Family GTPases* and *RHOA Signaling*, for the inhibited pathways, and *RHOGDI Signaling* as the top activated pathway. A summary of all pathways identified by IPA is provided in Supplementary Table 3.

Discussion

The lung is a major organ in constant direct contact with the external environment and thus, it has evolved to be unique in terms of cell metabolism, tissue organization, and immune responses (6,7). The alveolar lung mucosa is specialized with 3 main functions: maintenance of alveolar structure by preventing alveolar collapse, facilitation of gas exchange, and first line of defense against external insults which is the primary function of the ALF hypophase (1). We have demonstrated that ALF can shape responses to microbial infections (3,8), and those dysfunctional soluble proteins encountered in the older adult ALF are associated with worse infection outcomes, both in vitro and in vivo (2–4). Here, we investigated the proteome of

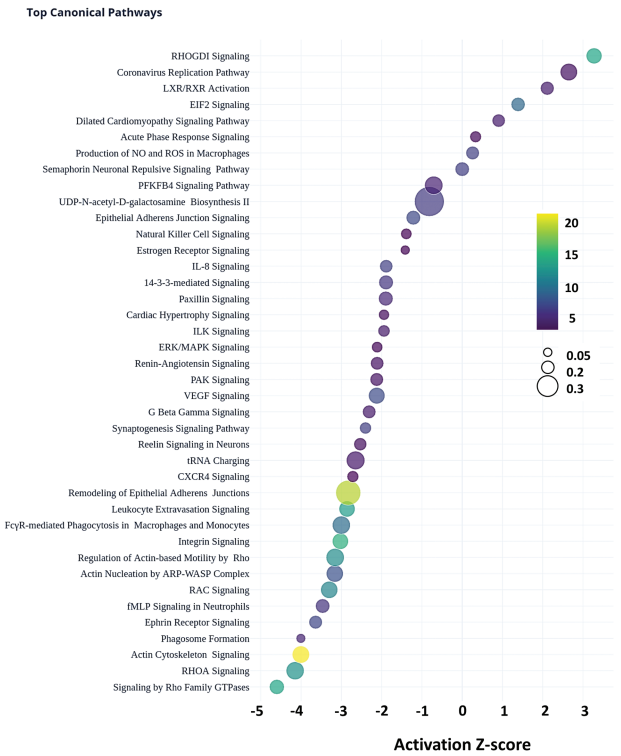

Figure 2. Top canonical pathways in the older adults. Top 40 canonical pathways of the DEPs. Pathway activation Z-scores, an inferred measurement of the pathway activation stated based on measured levels and IPA knowledge, is shown by bubble position on the x-axis (–4.146 to 3.273), Pathway name on the y-axis, -log-transformed *p*-values (color scale, blue-to-yellow, 4.02–22.8), and ratio (DEPs in data set belonging to pathway/proteins in the pathway for reference data set, bubble size, small-to-big, 0.0479–0.462).

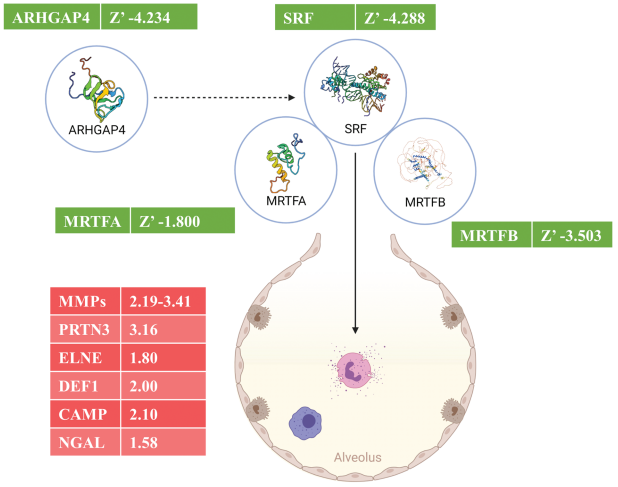

Figure 3. Predicted regulatory network in the older adults. A regulatory network showing the different proteins that could be playing a role in downstream effects of excess neutrophil degranulation in E-ALF. Each molecule is accompanied by higher detected $\log_2$ fold changes (red), or lower predicted activation Z-scores (green). Illustration created with BioRender (https://biorender.com/). ARHGAP4, Rho GTPase activating protein 4; SRF, serum response factor; MRTFA/B, myocardin-related transcription factor A/B; MMPs, matrix metalloproteinases; PRTN3, myeloblastin; ELNE, neutrophil elastase; DEF1, neutrophil defensin 1; CAMP, cathelicidin antimicrobial peptide; and NGAL, neutrophil gelatinase-associated lipocalin.

E-ALF versus A-ALF to understand age-related changes that occur in the soluble proteins of the alveoli and to gain insight into changes that may occur at the cellular level. Our results characterize proteins that are significant in their presence in the older adult ALF. Of relevance to this discussion, approximately 30% of proteins identified in the ALF (noncellular) compartment were considered of intracellular origin, but their source(s) remains unclear and needs to be further studied.

The significantly higher amounts of proteins of neutrophilic granule origin found in E-ALF (such as azurophil granule proteins-like proteinase 3; myeloperoxidase, elastase, and defensin-1a; and specific granule proteins-like cathelicidin and gelatinase-associated lipocalin) support the role of a neutrophilic contribution to the overall pro-inflammatory and pro-oxidation status of the alveolar mucosa in the older adult group. Indeed, neutrophils isolated from older adults have altered function and increase damage to tissues (9), and lungs of older adults harbor increased numbers of neutrophils (10). Thus, this neutrophil phenotype is consistent with higher degranulation in older adult individuals and could be one of the initiators of cellular senescence in the lungs (11). To further examine this, we looked for regulators that could drive this neutrophilic phenotype in the lungs of older adult individuals. Our IPA Causal Network Analysis assessing identified proteins of neutrophilic origin provided insight into a potential regulatory network orchestrated by the serum response factor (SRF, predicted *Z'* –4.288), predicted to be underproduced in the lungs of the older adults based on our downstream data. SRF is a transcription factor associated with neutrophil dysregulation, and our data suggest it is altered in older adults. Thus, we uncover a theoretical regulatory network for the neutrophil phenotype observed in our analysis, consisting of the main predicted regulator, SRF, together with its 2 cofactors, myocardin-related transcription factors A and B, and a predicted indirect regulator Rho GTPase activating protein 4 (ARHGAP4) (Figure 3).

A protein class detected at higher levels in E-ALF was the matrix metalloproteinase (MMP) family (Supplementary Tables 1 and 3) and their regulatory counterparts, the tissue inhibitors of matrix metalloproteinases (TIMPs). MMPs are a large family of Zn^{2+}- and Ca^{2+}-dependent endopeptidases produced by several cell types (12). Increased levels of MMPs strongly correlate with chronic inflammation and tissue destruction, hallmarks of lung catabolism and diseases (13). We detected 4 different MMPs, MMP-8, -9, and -10, significantly higher in the older adults (2.2, 3.41, and 2.19 $\log_2$ fold-change, respectively), and MMP-7, although not significant, showed a trend toward overproduction in older adults. We also detected TIMP1 (0.87, $\log_2$ fold-change), an MMP inhibitor that acts on all 4 detected MMPs. Although not statistically significant, the major inhibitor of MMP-9, α-2-macroglobulin, showed a trend toward overproduction. This profile of increased extracellular matrix remodeling suggests a chronic immunoinflammatory status of the lung of older adult individuals.

Lamin B1, a biomarker of cellular senescence, was also highly produced in E-ALF (Supplementary Table 1); however, its high production is opposite to other reports showing loss of Lamin B1 during aging (14–16). The Peptidoglycan Recognition Protein 1 (PGRP1) appeared significantly elevated in E-ALF. PGRP1 plays a bactericidal function in antimicrobial defense systems, acting as a pattern receptor for murein peptidoglycans (PGN) of gram-positive bacteria. Other proteins elevated ($p < .0005$) in E-ALF were IGHM (Immunoglobulin Heavy Constant Mu) and S100P (S100 Calcium Binding Protein P), both involved in early recognition of external

pathogens, including lung antimicrobial ciliary mobility and microvilli formation in lung epithelial cells. Interestingly, significantly elevated levels of eosinophil cationic protein (ECP, $p < .0005$) could further contribute to the inflammatory status of the aged lung. More pathways that were overrepresented in E-ALF are reported in Supplementary Table 3.

Pulmonary surfactant-associated proteins A and D (SFTPA and SFTPD, respectively) were lower in the E-ALF, although SFTPD was not significant. SFTPA and SFTPD are important initiators of the innate immune response, with lower levels associated with susceptibility to respiratory pathogens (3,4,17,18). Other proteins lower in E-ALF (Supplementary Table 2) were THMS2, a macrophage immunomodulator of B cell responses thought to increase the sensitivity of immature B cells to rare and low-affinity antigens through PLCG2, which was also found to be significantly lower in the older adults (19,20). Caveolin-1 (CAV1), significantly reduced in the E-ALF, is necessary for caveolae formation, an endocytic and transcytic clearance and signaling network present in some lung cells (21). Downregulation of CAV1 is linked to inflammasome activation (22) and results in different pulmonary disease states, including inflammatory diseases (21). Related to this, EH domain-containing protein 2 (EHD2) was also lower in the E-ALF (23), as well as dynamins 1 and 2 (DNM1L and DYN2) (24–26). Another protein significantly lower in E-ALF was PACN2, which is activated by dynamin 1, further indicating dysregulation of immature B cells (19,20). Coiled-coil domain-containing protein 93 (CCD93), involved in endosome recycling (27), was also significantly lower.

Overall, we performed a proteomic analysis comparing E-ALF versus A-ALF composition and discussed some of the significantly altered proteins and potential pathways implicated. Our data reported herein should serve as a baseline to understand the biochemical changes that occur in the alveolar mucosa as we age. The importance of this understudied area is highlighted by the fact that life expectancy will increase during this century (forecasted to be over 100 years old by year 2100, in high-income countries).

Methods

Human Subjects and Ethics Statement

Human subject studies were carried out following the U.S. Code of Federal and Local Regulations (The Ohio State University IRB#: 2008H0135/2008H0119 and Texas Biomedical Research Institute/UT-Health San Antonio/South Texas Veterans Health Care System IRB#: HSC20170667H). Bronchoalveolar lavage (BAL) fluid was obtained and processed within 6 h from well-characterized adult (aged 23–48 years, female:male ratio of 33%:67%) and older adult (aged 62–73 years, female:male ratio of 50%:50%) without discrimination of race or ethnicity after informed written consent. BAL fluid was obtained on healthy-appearing lung segments (as predetermined by X-rays and the pulmonologist) of donors during an exploratory BAL due to the suspicion of having a nodule in their lungs (2,3). At the time of performing the BAL, donors did not present any clinical symptom, and their blood biochemistry, respiratory function, lung capacity (spirometry) values were within the normal range as a healthy person. Donors that were smokers; injection/noninjection drug and/or excessive alcohol users; or those with acute pneumonia, upper/lower respiratory tract infections, any kind of acute illness/chronic condition, heart disease, diabetes, asthma, chronic sinusitis/bronchitis, chronic obstructive pulmonary disease, renal failure, liver failure, hepatitis, thyroid disease, rheumatoid arthritis, immunosuppression or taking nonsteroidal anti-inflammatory agents, human immunodeficiency virus (HIV)/AIDS, cancer requiring chemotherapy, leukemia/lymphoma, seizure history, blood disorders, lidocaine allergies (used during the BAL), pregnancy, nontuberculous mycobacterial infections, and TB were excluded as described (2,3).

BAL Fluid Processing to Obtain ALF

BAL fluid was collected and concentrated to obtain the ALF as described (3,4,8).

Proteomic Analyses

ALF samples were mixed with 5% sodium dodecyl sulfate/50 mM triethylammonium bicarbonate (TEAB) and protease and phosphatase inhibitors (Halt; Thermo-Scientific). Proteins (50 µg, by EZQ Protein Quantitation Kit; Thermo-Scientific) were reduced with Tris(2-carboxyethyl) phosphine hydrochloride, alkylated in the dark with iodoacetamide, and applied to S-Traps (micro; Protifi) for tryptic digestion (sequencing grade; Promega) in 50 mM TEAB. Peptides were eluted with 0.2% formic acid in 50% aqueous acetonitrile and quantified using Pierce Quantitative Fluorometric Peptide Assay (Thermo-Scientific).

DIA-MS was conducted on an Orbitrap Fusion Lumos (Thermo-Scientific). On-line HPLC separation used a RSLC NANO column (Thermo-Scientific/Dionex: column, PicoFrit [New Objective; 75 µm i.d.]) packed to 15 cm with C18 adsorbent (Vydac; 218MS 5 µm, 300 Å); mobile phase A, 0.5% acetic acid (HAc)/0.005% trifluoroacetic acid (TFA) in water; mobile phase B, 90% acetonitrile/0.5% HAc/0.005% TFA/9.5% water; gradient 3%–42% B in 120 minutes; flow rate, 0.4 µL/min. From pooled samples, 1-µg peptide aliquots were analyzed using gas-phase fractionation and 4-*m/z* windows (30k resolution for precursor and product ion scans, all in the Orbitrap) to create a DIA chromatogram library by searching against a Prosit-generated predicted spectral library based on the UniProt_human_20191022 database. Experimental samples were randomized for sample preparation and analysis. Injections of 1-µg of peptides were employed. MS data for experimental samples were acquired in the Orbitrap using 8-*m/z* windows (staggered; 30k resolution for precursor and product ion scans) and searched against the chromatogram library. Scaffold DIA (vr.3.0.0; Proteome Software) was used for all DIA data processing.

Data Statistical Analyses

DEPs were selected based on the following thresholds, $\log_2$ fold-change < -0.5 or > 0.5, p-value $< .055$ as given by Benjamini–Hochberg multiple testing correction of false discovery rate set at 20%. Plotly Dash Chart was used to generate bar and bubble charts. DEPs were annotated using the 2021-08-18 release of Human GOA (Gene Ontology Consortium). IPA (v65367011; QIAGEN) was used to perform pathway analysis and regulator prediction analyses.

Supplementary Material

Supplementary data are available at *The Journals of Gerontology, Series A: Biological Sciences and Medical Sciences* online.

Supplementary Table 1. Detailed $\log_2$-transformed fold changes for higher DEPs in the older adults. Proteins significantly higher in E-ALF vs. A-ALF. *p<0.05; **p<0.005; ***p<0.0005; ****p<0.0001, ANOVA with Benjamini–Hochberg control of FDR at 20%. Highlighted darker lines in for lower p-value group.

Supplementary Table 2. Detailed $\log_2$-transformed fold changes for lower DEPs in the older adults. Proteins significantly lower in E-ALF vs. A-ALF. *p<0.05; **p<0.005; ***p<0.0005; ****p<0.0001, ANOVA with Benjamini–Hochberg control of FDR at 20%. Highlighted darker lines in for lower p-value group.

Supplementary Table 3. Canonical pathways. A table with all (417) significantly enriched Canonical Pathways identified by IPA analysis, showing -log(p-value) of the protein overlap, a ratio of DEPs in dataset belonging to pathway/Proteins in pathway for reference dataset, and an activation z-score, an estimation of the overall activation of the pathway based on the status of the molecules identified in E-ALF.

Supplementary Figure 1. Gene Ontology annotations, distribution of proteins in the older adults. Top: Stacked bar chart of the total number of significant proteins identified by DIA-MS in the E-ALF [blue (lower relative quantification) and red (Higher relative quantification)] belonging to the different GO classifications (Biological Process, Cellular Component, and Molecular Function). Bottom: Stacked bar chart of the total number of all the proteins identified by DIA-MS in the E-ALF [blue (Lower relative quantification) and red (Higher relative quantification)] belonging to the different GO classifications (Biological Process, Cellular Component, and Molecular Function).

Funding

Supported by National Institutes of Health/National Institute on Aging (NIH/NIA) P01AG051428 award to J.T., J.B.T, L.S.S., and B.I.R. The Robert J. Kleberg, Jr. and Helen C. Kleberg Foundation partially supported J.B.T. The Douglass Graduate Fellowship supported A.M.O.-F.

Conflict of Interest

None declared.

Acknowledgments

MS analyses were conducted in the Institutional MS Laboratory of the UT-Health SA, with support from UT-Health SA for the laboratory and the University of Texas System for purchase of the Orbitrap Fusion Lumos MS. We thank Mr. Pardo and Ms. Molleur for MS technical support, and Drs. Headley and Piergallini for IPA software assistance.

Author Contributions

A.G.-V. data analysis; A.G.-V., A.M.O.-F., J.I.M., A.A.-G, sample processing; H.S., R.E.M., D.J.M., J.I.P. procured samples; Y.W., J.B.T. reviewed data analysis; S.T.W. DIA-MS data analysis; A.G.-V. and J.B.T. study conceptualization, experimental design, wrote the manuscript; B.I.R., Y.W., S.T.W., L.S.S., J.T. critically reviewed the manuscript. B.I.R., L.S.S., J.T., and J.B.T. provided funding. All authors read and approved the final version of this manuscript.

Data Availability

Data supporting findings are available in Supplementary Materials. Raw Mass Spectrometry files and the Data-Independent Acquisition file are publicly available at MassIVE (ProteomeXchange consortium), under accession number PXD033088.

References

1. Fronius M, Clauss W, Althaus M. Why do we have to move fluid to be able to breathe? *Front Physiol.* 2012;3:146. doi:10.3389/fphys.2012.00146
2. Moliva JI, Rajaram MV, Sidiki S, et al. Molecular composition of the alveolar lining fluid in the aging lung. *Age (Dordr)* 2014;36:9633. doi:10.1007/s11357-014-9633-4
3. Moliva JI, Duncan MA, Olmo-Fontánez A, et al. The lung mucosa environment in the elderly increases host susceptibility to *Mycobacterium tuberculosis* infection. *J Infect Dis.* 2019;220:514–523. doi:10.1093/infdis/jiz138
4. Olmo-Fontánez AM, Scordo JM, Garcia-Vilanova A, Maselli DJ, Peters JI, Restrepo BI, et al. Human alveolar lining fluid from the elderly promotes *Mycobacterium tuberculosis* growth in alveolar epithelial cells and bacterial translocation into the cytosol. *bioRxiv*. 2021. doi:10.1101/2021.05.12.443884
5. Diz AP, Carvajal-Rodríguez A, Skibinski DO. Multiple hypothesis testing in proteomics: a strategy for experimental work. *Mol Cell Proteomics*. 2011;10:M110.004374. doi:10.1074/mcp.M110.004374
6. Guillot L, Nathan N, Tabary O, et al. Alveolar epithelial cells: master regulators of lung homeostasis. *Int J Biochem Cell Biol.* 2013;45:2568–2573. doi:10.1016/j.biocel.2013.08.009
7. Hussell T, Bell TJ. Alveolar macrophages: plasticity in a tissue-specific context. *Nat Rev Immunol.* 2014;14:81–93. doi:10.1038/nri3600
8. Arcos J, Sasindran SJ, Moliva JI, et al. *Mycobacterium tuberculosis* cell wall released fragments by the action of the human lung mucosa modulate macrophages to control infection in an IL-10-dependent manner. *Mucosal Immunol.* 2017;10:1248–1258. doi:10.1038/mi.2016.115
9. Drew W, Wilson DV, Sapey E. Inflammation and neutrophil immunosenescence in health and disease: targeted treatments to improve clinical outcomes in the elderly. *Exp Gerontol.* 2018;105:70–77. doi:10.1016/j.exger.2017.12.020
10. Meyer KC, Ershler W, Rosenthal NS, Lu XG, Peterson K. Immune dysregulation in the aging human lung. *Am J Respir Crit Care Med.* 1996;153:1072–1079. doi:10.1164/ajrccm.153.3.8630547
11. Lagnado A, Leslie J, Ruchaud-Sparagano M-H, et al. Neutrophils induce paracrine telomere dysfunction and senescence in ROS-dependent manner. *EMBO J.* 2021;40:e106048. doi:10.15252/embj.2020106048
12. Burgstaller G, Oehrle B, Gerckens M, White ES, Schiller HB, Eickelberg O. The instructive extracellular matrix of the lung: basic composition and alterations in chronic lung disease. *Eur Respir J.* 2017;50:16018051601805. doi:10.1183/13993003.01805-2016
13. Greenlee KJ, Werb Z, Kheradmand F. Matrix metalloproteinases in lung: multiple, multifarious, and multifaceted. *Physiol Rev.* 2007;87:69–98. doi:10.1152/physrev.00022.2006
14. Garvalov BK, Muhammad S, Dobreva G. Lamin B1 in cancer and aging. *Aging (Albany NY)* 2019;11:7336–7338. doi:10.18632/aging.102306
15. Freund A, Laberge RM, Demaria M, Campisi J. Lamin B1 loss is a senescence-associated biomarker. *Mol Biol Cell.* 2012;23:2066–2075. doi:10.1091/mbc.E11-10-0884
16. Saito N, Araya J, Ito S, et al. Involvement of Lamin B1 reduction in accelerated cellular senescence during chronic obstructive pulmonary disease pathogenesis. *J Immunol.* 2019;202:1428–1440. doi:10.4049/jimmunol.1801293
17. LeVine AM, Kurak KE, Bruno MD, Stark JM, Whitsett JA, Korfhagen TR. Surfactant protein-A-deficient mice are susceptible to *Pseudomonas aeruginosa* infection. *Am J Respir Cell Mol Biol.* 1998;19:700–708. doi:10.1165/ajrcmb.19.4.3254
18. van Eijk M, Rynkiewicz MJ, Khatri K, et al. Lectin-mediated binding and sialoglycans of porcine surfactant protein D synergistically neutralize influenza A virus. *J Biol Chem.* 2018;293:10646–10662. doi:10.1074/jbc.ra117.001430
19. Deobagkar-Lele M, Anzilotti C, Cornall RJ. Themis2: setting the threshold for B-cell selection. *Cell Mol Immunol.* 2017;14:643–645. doi:10.1038/cmi.2017.27
20. Cheng D, Deobagkar-Lele M, Zvezdova E, et al. Themis2 lowers the threshold for B cell activation during positive selection. *Nat Immunol.* 2017;18:205–213. doi:10.1038/ni.3642
21. Maniatis NA, Chernaya O, Shinin V, Minshall RD. Caveolins and lung function. *Adv Exp Med Biol.* 2012;729:157–179. doi:10.1007/978-1-4614-1222-9_11

22. Lin X, Barravecchia M, Matthew Kottmann R, Sime P, Dean DA. Caveolin-1 gene therapy inhibits inflammasome activation to protect from bleomycin-induced pulmonary fibrosis. *Sci Rep*. 2019;9:19643. doi:10.1038/s41598-019-55819-y
23. Mohan J, Morén B, Larsson E, Holst MR, Lundmark R. Cavin3 interacts with cavin1 and caveolin1 to increase surface dynamics of caveolae. *J Cell Sci*. 2015;128:979–991. doi:10.1242/jcs.161463
24. Lamsoul I, Dupré L, Lutz PG. Molecular tuning of filamin A activities in the context of adhesion and migration. *Front Cell Dev Biol*. 2020;8. doi:10.3389/fcell.2020.591323
25. Millán J, Cain RJ, Reglero-Real N, et al. Adherens junctions connect stress fibres between adjacent endothelial cells. *BMC Biol*. 2010;8:11. doi:10.1186/1741-7007-8-11
26. Mitchell LA, Ward C, Kwon M, et al. Junctional adhesion molecule A promotes epithelial tight junction assembly to augment lung barrier function. *Am J Pathol*. 2015;185:372–386. doi:10.1016/j.ajpath.2014.10.010
27. Wang J, Fedoseienko A, Chen B, Burstein E, Jia D, Billadeau DD. Endosomal receptor trafficking: retromer and beyond. *Traffic* 2018;19:578–590. doi:10.1111/tra.12574